

On fiber flocculation in turbulent pulp flow

Mats S. Nigam

Noss AB, P.O. Box 20, 601 02 Norrköping, Sweden

ABSTRACT

Fundamental ideas on the interaction between fibers in turbulent flow are presented. In stationary homogeneous turbulence, there is a high probability of floc formation whereas in shear-flow turbulence or in turbulent straining motion, flocs are less likely to form and may even rupture. The phenomenological results are used to formulate a leading-order model for flocculation in developing pipe flow.

INTRODUCTION

In the pulp and paper industry, the high process rates produce turbulent flow nearly everywhere in the system. The stirring character of the turbulent flow causes fiber entanglement, resulting in the formation of local fiber aggregates (flocs) which produce irregularities in strength and opacity of the final product. There is thus an urgent need for models which accurately predict the rate of floc formation in turbulent flow. The aim of the present study is to provide a basic understanding of the underlying phenomena. Results from classical turbulence theory are used to assess the qualitative behavior of fibers in elementary turbulent flow fields. The conclusions are used to formulate a leading-order model for flocculation in developing pipe flow.

TURBULENCE ENERGY-SPECTRUM OF A FIBER SUSPENSION

Turbulence is characterized by eddying motion with an energy-cascade in which

energy is transferred from large scales to smaller and smaller scales until it reaches the so-called Kolmogorov scale. At this length-scale, the action of viscosity effectively dissipates the remaining energy. The energy-cascade is schematically visualized in Fig. 1 below.

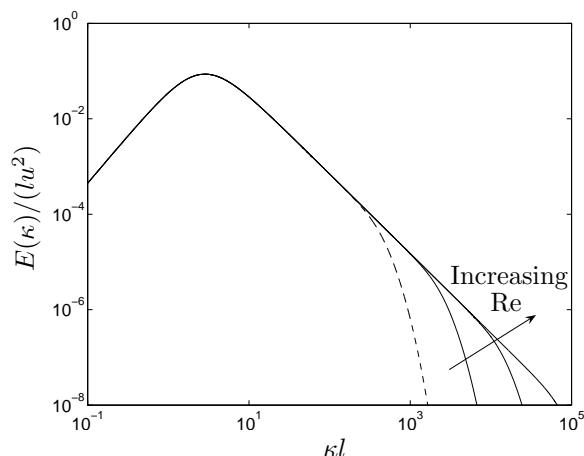


Figure 1. Turbulence energy spectra for three different values of the Reynolds number (solid curves). The modified energy-spectrum of a turbulent fiber suspension is shown as the dashed curve.

The normalized energy is plotted against κl , where κ is the wave-number and l is the size of the energy-containing eddies (defined by $l = u^3/\epsilon$, where ϵ is the dissipation of turbulent kinetic energy and u is the velocity-scale of the energy-containing eddies). Energy-spectra are shown for three different values of the Reynolds number. As the Reynolds number increases the Kolmogorov scale decreases. This is shown in Fig. 1 as an increase in the wave-number at which the

curves start to descend more rapidly. An important characteristic of turbulent fiber suspensions is that the presence of fibers enhances the decay-rates of turbulent eddies with length-scales smaller than the fiber length. Also shown in Fig. 1 is a modified spectrum (dashed curve) with a larger cut-off length (the point at which the curve starts to descend more rapidly) due to the presence of fibers. Unlike the Kolmogorov cut-off length, the fiber-induced cut-off length is independent of the Reynolds number. If the Reynolds number were small, such that the Kolmogorov length is larger than the fiber cut-off length, turbulent dissipation would be unaffected by the presence of fibers. In most cases pertaining to pulp-processing the Reynolds number will be large enough for the dissipation to be entirely controlled by the fiber cut-off length. Duffy and Lee¹ measured the friction factor for various pulp consistencies in pipe flow and observed it to be constant for a range of Reynolds numbers just above the point of maximum drag reduction. At yet higher Reynolds numbers, the friction factor appeared to approach values corresponding to pure water.

THE INTERACTION BETWEEN FIBERS IN TURBULENT FLOW

In order to understand the effect of turbulence on suspended fibers, it is instructive to consider a “tagged” fluid particle as it moves around in the flow field. Consider first the motion of a fluid particle in stationary (statistically steady), homogeneous turbulence. We note in passing that such a flow can not be sustained since mean shear is needed for turbulent production. Hence, the turbulence would be in a state of decay and this violates the assumption of stationarity. In many bounded turbulent flows there are regions in the interior of the flow field where

the turbulence is approximately stationary and homogeneous, and to which energy is supplied from regions of turbulent production in close proximity to the outer boundaries. The following discussion is restricted to such regions of the flow field. If the position of a particle at $t = 0$ is \mathbf{x}_0 , it is possible to show² that the mean distance between the particle at time t and its original position is proportional to \sqrt{t} ,

$$|\langle \mathbf{x}(t) - \mathbf{x}_0 \rangle| \sim \sqrt{t}, \quad (1)$$

where $\langle \dots \rangle$ denotes a spatial average. On the other hand, the length of the path traced out by the particle must be proportional to t . The particle may be thought of as performing a random walk as shown in Fig. 2.

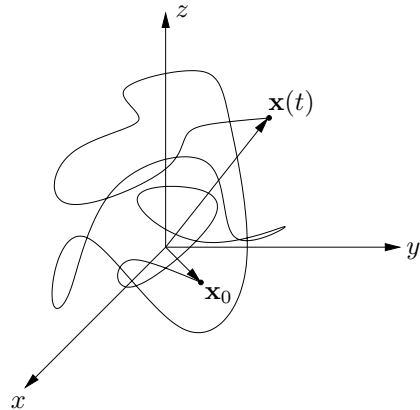


Figure 2. The motion of a wandering point in stationary, homogeneous turbulence

Next, consider a single fiber, performing a random walk in a homogeneous turbulent flow field. Since the distance between the end-points of the fiber is restricted by its length, the fiber will twist and fold around its principal axes. In a fiber suspension, each fiber traces out a path with length proportional to t whereas the distance between the centers of mass of two individual fibers only grows as \sqrt{t} . Hence, there is a large probability that two fibers which are initially close together will

interact and become entangled before the distance between their centers of mass has grown large enough for their end-points to have moved out of reach of one another. Similarly, an isolated fiber bundle consisting of interlocked fibers would become more and more entangled and its network strength would increase at the cost of the kinetic energy of the turbulent flow field. A fiber bundle in an otherwise homogeneous fiber suspension would in addition grow as more and more fibers become interlocked with the bundle.

A simple experiment illustrating these observations is described by Fellers and Norman³. Dry, non-flocculated fibers are carefully added to a beaker initially filled with pure water until the concentration of fibers well exceeds the sediment concentration. When a spoon is placed vertically at the center of the beaker it immediately falls to the rim. Next, turbulent energy is added to the suspension by a mechanical stirrer. After that, when the spoon is placed at the center of the beaker, it stands upright supported by the fiber network. Thus, the turbulent kinetic energy has been transformed into fiber network strength (and heat).

In summary, we may conclude that *stationary, homogeneous turbulence enhances flocculation*.

A different scenario is expected to occur when the turbulence is anisotropic. In a uniform shear flow with mean velocities $(U, V, W) = (Sy, 0, 0)$ in the x , y and z directions respectively, fluid particles separate faster in the stream-wise direction and it is possible to show⁴ that,

$$\begin{aligned} | \langle x(t) - \bar{x}(t) \rangle | &\sim t^{3/2}, \\ | \langle y(t) - y(0) \rangle | &\sim \sqrt{t}, \\ | \langle z(t) - z(0) \rangle | &\sim \sqrt{t}, \end{aligned} \quad (2)$$

where the separation in the stream-wise direction is measured relative to the mean

displacement of fluid particles, $\bar{x}(t)$, due to the mean flow. Hence, the inter-particle separation distance in the stream-wise direction grows faster ($\sim t^{3/2}$) than the length of the path traced out by individual fibers ($\sim t$). As a result of this, there is a possibility for fiber bundles (or flocs) to be pulled apart in turbulent shear flows. Similarly, in a 2D straining motion, $(U, V, W) = (Sx, -Sy, 0)$, which can be obtained by passage of the flow through a smooth contraction, the stream-wise particle separation is expected to grow as e^{St} which is even faster than in uniform shear flow. In this case however, the stream-wise stretching is accompanied by a cross-stream compression as well as an increase in stream-wise vorticity (local spin about the x -axis). These effects may induce a growth in network strength and enhance the rate of entanglement. The net effect of a mean strain is however positive for floc rupturing as shown in the experiments by Kerekes⁵.

From the previous paragraph, we may conclude that *mean shear and mean strain enhance de-flocculation in turbulent flow*.

FLOCCULATION IN DEVELOPING PIPE FLOW

The ideas presented in the previous section naturally lead to the notion of a yield stress, τ_y . At high concentrations, all fibers are locked into a global network which must be disrupted in order to produce a flow. Hence, concentrated fiber suspensions are expected to behave as yield-stress fluids. In the intermediate range, where the concentration is too low to produce a global network, any kind of stirring motion will potentially lead to entanglement and the production of local aggregates (flocs) provided the local shear stress is smaller than τ_y . As initially de-flocculated pulp passes through a pipe, a certain level of flocculation occurs due to the stirring mo-

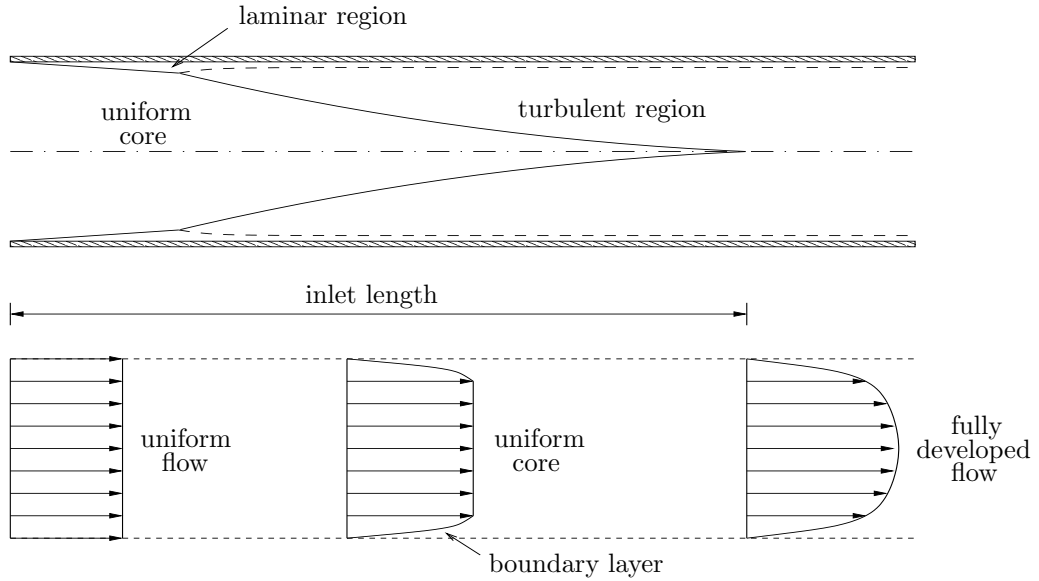


Figure 3. Schematic of developing pipe flow

tion produced by the turbulent eddies in the boundary layer and eventually in the fully developed turbulent pipe-flow profile. While the complex details of the flocculation process are poorly understood, the qualitative behavior can be analyzed with simple scaling laws which are presented herein to obtain leading-order estimates for the level of re-flocculation in developing pipe flow.

When a uniform flow enters a straight circular pipe, the flow evolves into a velocity distribution which is independent of the distance from the inlet. The final velocity distribution is called the fully developed profile and the distance between the inlet and the point at which the fully developed profile is established is called the inlet length. At high Reynolds numbers ($\text{Re} = \bar{u}a/\nu$, where \bar{u} is the mean velocity, a the radius of the pipe and ν the kinematic viscosity) the initially laminar boundary layer at the pipe wall destabilizes and becomes turbulent a short distance from the entrance. The boundary layer grows radially inward until it fills the whole cross-section, at which point the fi-

nal velocity profile is established (see Fig. 3). In fully developed pipe flow, the shear stress varies linearly from the value, τ_w , at the wall to zero at the center of the pipe,

$$\tau(y) = \left(1 - \frac{y}{a}\right)\tau_w, \quad (3)$$

where y is measured from the pipe wall (see Fig. 4).

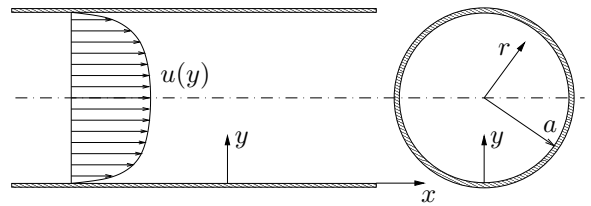


Figure 4. The fully developed velocity profile shown together with reference to the coordinate axes

It will be assumed that this relation holds also in the evolving boundary layer upstream of the fully developed profile,

$$\tau(x, y) = \left(1 - \frac{y}{\delta(x)}\right)\tau_w(x), \quad (4)$$

where $\delta(x)$ is the local boundary-layer thickness and $\tau_w(x)$ is the local shear stress

at the wall. Given the yield stress, τ_y , and assuming that the relation given in Eq. 4 is applicable, a few interesting phenomena may readily be deduced.

At a distance, x , downstream of the inlet there is a turbulent boundary layer of width $\delta(x)$ next to the wall and a uniform laminar core which as of yet is uninfluenced by the turbulent motion close to the wall. Flocculation will occur in the turbulent part of the flow field where $\tau < \tau_y$,

$$\begin{aligned} \tau_w(x) \left(1 - \frac{y}{\delta(x)}\right) &< \tau_y, \quad \text{with } y/\delta(x) < 1 \\ \Rightarrow \frac{\delta(x)}{a} \left(1 - \frac{\tau_y}{\tau_w(x)}\right) &< \frac{y}{a} < \frac{\delta(x)}{a}. \end{aligned} \quad (5)$$

Substituting $r = a - y$ for the radial coordinate, it is found that fiber flocs are formed within a ring-shaped region of the pipe cross-section,

$$1 - \frac{\delta(x)}{a} < \frac{r}{a} < 1 - \frac{\delta(x)}{a} \left(1 - \frac{\tau_y}{\tau_w(x)}\right). \quad (6)$$

The outer boundary of the flocculated region is given by the radial location inside the turbulent boundary layer at which the shear stress first falls below the yield stress, and the inner boundary of the ring-shaped region is given by the radius of the uniform laminar core. As the laminar core diminishes downstream, the flocculated region becomes circular in the fully developed flow. If $\tau_w(l) > \tau_y$, where l is the inlet length, there will be a layer free from flocs next to the wall in the fully developed flow (see Fig. 5). Contrary, if $\tau_w(l) < \tau_y$, the entire flow field will become flocculated. The ratio of the flocculated area to the cross-section of the pipe as a function of x is given by,

$$\begin{aligned} A(x) &= \left[1 - \frac{\delta}{a} \left(1 - \frac{\tau_y}{\tau_w}\right)\right]^2 - \left(1 - \frac{\delta}{a}\right)^2 = \\ &= 2 \frac{\delta}{a} \left(1 - \frac{\delta}{a}\right) \frac{\tau_y}{\tau_w} + \left(\frac{\delta}{a}\right)^2 \left(\frac{\tau_y}{\tau_w}\right)^2. \end{aligned} \quad (7)$$

If $\tau_y > \tau_w(l)$, Eq. 7 only applies for $x \leq x_c$ where $x_c : \tau_w(x_c) = \tau_y$. Downstream of x_c the ratio of the flocculated area to the cross-section of the pipe is given by,

$$A(x) = 2 \frac{\delta(x)}{a} - \left(\frac{\delta(x)}{a}\right)^2. \quad (8)$$

Eq. 7 and Eq. 8 require knowledge about τ_y , $\tau_w(x)$ and $\delta(x)$. Measurements of the yield stress in various fiber suspensions have been obtained by Kerekes et al⁶ and Bennington et al⁷. $\tau_w(x)$ and $\delta(x)$ can be estimated from scaling laws and empirical correlations. Assuming that the Reynolds number is large, the extent of the laminar part of the boundary layer close to the entrance (see Fig. 3) becomes negligible compared to the full inlet length. Let the velocity distribution in the boundary layer be described by,

$$\begin{aligned} \frac{u(x, y)}{u_*(x)} &= C(n) \left(\frac{u_*(x)y}{\nu}\right)^{1/n}, \\ \text{with } u_*(x) &= \sqrt{\frac{\tau_w(x)}{\rho}}, \end{aligned} \quad (9)$$

where $u_*(x)$ is the friction velocity, n is a number ≥ 7 and $C(n)$ is a constant depending on the choice of n . At the edge of the boundary layer, $y = \delta(x)$, the velocity must be equal to that of the uniform core, $U(x)$,

$$\frac{U(x)}{u_*(x)} = C(n) \left(\frac{u_*(x)\delta(x)}{\nu}\right)^{1/n}. \quad (10)$$

Combining Eq. 9 and Eq. 10,

$$\frac{u(x, y)}{U(x)} = \left(\frac{y}{\delta(x)}\right)^{1/n}. \quad (11)$$

The core velocity, $U(x)$, may be related to the mean velocity, \bar{u} , by imposing continuity,

$$\begin{aligned} \frac{\bar{u}}{U} &= 1 - \frac{3n+1}{(2n+1)(n+1)} \frac{\delta}{a} \\ &\quad - \frac{1}{2n+1} \frac{\delta}{a} \left(1 - \frac{\delta}{a}\right). \end{aligned} \quad (12)$$

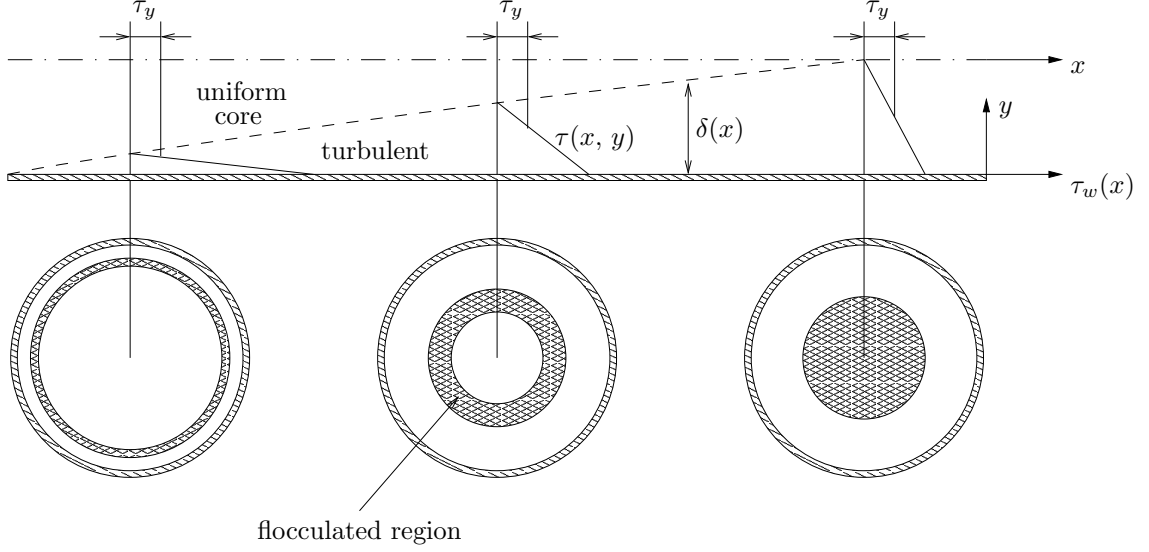


Figure 5. A ring-shaped region of flocculated flow, externally bounded by the radius for which $\tau(x, y) = \tau_y$ and internally by the boundary layer thickness, evolves into a circular flocculated region in the fully developed flow

Estimates for $\tau_w(x)$ and $\delta(x)$ can now be obtained by inserting the above relations into von Karman's integral equation,

$$(2\delta_2 + \delta_1) U \frac{dU}{dx} + U^2 \frac{d\delta_2}{dx} = \frac{\tau_w}{\rho}, \quad (13)$$

where the displacement thickness and the momentum thickness are given by,

$$\delta_1 = \int_0^\delta \left(1 - \frac{u}{U}\right) \left(1 - \frac{y}{a}\right) dy, \quad (14)$$

$$\delta_2 = \int_0^\delta \frac{u}{U} \left(1 - \frac{u}{U}\right) \left(1 - \frac{y}{a}\right) dy. \quad (15)$$

Then, to leading order,

$$\delta^{2/(n+1)} d\delta \sim \left(\frac{\nu}{\bar{u}}\right)^{2/(n+1)} dx \Rightarrow \delta(x) \sim \left(\frac{\nu}{\bar{u}x}\right)^{2/(n+3)} x, \quad (16)$$

and,

$$\frac{\tau_w(x)}{\frac{1}{2}\rho\bar{u}^2} \sim \left(\frac{\nu}{\bar{u}x}\right)^{2/(n+3)}. \quad (17)$$

Using,

$$\delta(x) = C_\delta \left(\frac{\nu}{\bar{u}x}\right)^{2/(n+3)} x, \quad (18)$$

with $\delta(l) = a$ gives the following expression for the inlet length,

$$\frac{l}{a} = C_\delta^{-(n+3)/(n+1)} \left(\frac{\bar{u}a}{\nu}\right)^{2/(n+1)}. \quad (19)$$

Comparing this to the empirical correlation,

$$\frac{l}{a} = 8.8 \text{Re}^{1/6} = 8.8 \left(\frac{\bar{u}a}{\nu}\right)^{1/6}, \quad (20)$$

it is found that,

$$n = 11 \quad \text{and} \quad C_\delta = 0.16. \quad (21)$$

With $n = 11$, the wall shear stress and the boundary-layer thickness are given by,

$$\frac{\tau_w(x)}{\tau_w(l)} = \left(\frac{l}{x}\right)^{1/7} \quad \text{and} \quad \frac{\delta(x)}{a} = \left(\frac{x}{l}\right)^{6/7}. \quad (22)$$

Eq. 7 may now be expressed in the following form,

$$A(X) = 2X(1 - X^{6/7})T + X^2T^2, \quad (23)$$

for $0 \leq X \leq 1$ where,

$$X = x/l \quad \text{and} \quad T = \tau_y/\tau_w(l). \quad (24)$$

If $T > 1$, Eq. 23 is valid up to $X = X_c = T^{-7}$. For $X > T^{-7}$, the ratio of the flocculated area to the cross-section of the pipe is given by Eq. 8,

$$A(X) = 2X^{6/7} - X^{12/7}, \quad (25)$$

for $T > 1$, $X > T^{-7}$. The ratio of flocculated flux to total flux at the downstream location X is given by,

$$\begin{aligned} \frac{Q_f(X)}{Q} &= \frac{\int_{\delta(1-\frac{\tau_y}{\tau_w})}^{\delta} U\left(\frac{y}{\delta}\right)^{1/n} (a-y) dy}{\int_0^a U\left(\frac{y}{\delta}\right)^{1/n} (a-y) dy} \\ &= A(X) + O\left(\frac{1}{n}\right) \approx A(X), \end{aligned} \quad (26)$$

where the last approximation is justified by the level of approximation in the preceding analysis. Fig. 6 displays the ratio of flocculated flux to total flux for different values of $T = \tau_y/\tau_w(l)$. The curves for

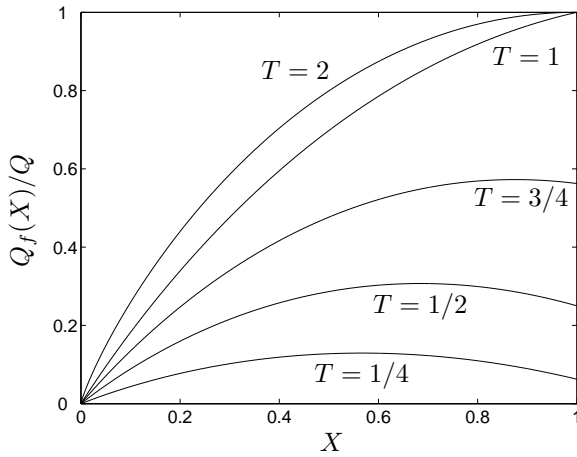


Figure 6. Ratio of flocculated flux to total flux as given by Eq. 26 for different values of T

larger values of T are hardly distinguishable from the curve $T = 2$. An interesting observation from Fig. 6 is that the curves are non-monotonic for $T \lesssim 3/4$. In order to use the graph, it is necessary to first

obtain the appropriate value of T . Bennington et al⁷ give empirical correlations for the yield stress on the form,

$$\tau_y = K_1 C^{K_2}, \quad (27)$$

where K_1 and K_2 are constants specific to the type of fibers in the suspension, and C is the concentration. A somewhat more physically based correlation is given by Martinez et al⁸,

$$\tau_y = 5.5 \times 10^{-4} (N - N_{gel})^{2.3}, \quad (28)$$

where $N = \pi C_m L_f^2 / 6\omega$ is the crowding number, $N_{gel} = 16$ is the crowding number at which flocs start to form, C_m is the concentration in $[\text{kg}/\text{m}^3]$, L_f in $[\text{m}]$ is an interaction length based on the fiber length, and ω is the coarseness in $[\text{kg}/\text{m}]$. Both correlations produce rather crude estimates of the yield stress, and should be updated as more accurate data becomes available. In a flocculated suspension, the concentration within the flocs will be higher than that in between flocs. This must be taken into account when estimating the disruptive floc yield stress. An upper bound on the average floc concentration can be obtained by assuming that all fibers are locked into disjoint closely packed spherical flocs of equal size,

$$C_{mf} \leq \frac{8}{\pi\sqrt{3}} C_m \approx 1.47 C_m. \quad (29)$$

This upper bound is consistent with the experimental values 1.26–1.44 reported by Ringnér⁹. Hence, the disruptive floc yield stress can be estimated from,

$$\begin{aligned} \tau_y &= 5.5 \times 10^{-4} \left(\frac{\pi C_{mf} L_f^2}{6\omega} - N_{gel} \right)^{2.3} \\ &\approx 5.5 \times 10^{-4} \left(\frac{C_m L_f^2}{1.3\omega} - 16 \right)^{2.3} \quad [\text{Pa}]. \end{aligned} \quad (30)$$

The wall shear stress, $\tau_w(l)$, in fully developed pipe flow is given by,

$$\tau_w(l) = \frac{1}{2} \rho \bar{u}^2 \tau^*, \quad (31)$$

where the dimensionless wall stress, τ^* , is obtained from Prandtl's universal friction law,

$$\frac{1}{\sqrt{\tau^*}} = 4.0 \log_{10}(\text{Re} \sqrt{\tau^*}) + 0.81. \quad (32)$$

The empirical correlations in Eq. 20 and 32 apply to pure water and should be replaced by the proper expressions for a specific pulp as such data becomes available. Thereby, the attenuating effect of fibers on the small-scale turbulence may be captured to leading order. Given the Reynolds number, fiber concentration, length and coarseness, the value of T can be estimated from Eq. 30, 31 and 32. The level of re-flocculation as a function of the distance from the inlet is then obtained from Fig. 6.

CONCLUSION

Results from classical turbulence theory and experimental observations were used to assess the qualitative behavior of fibers in elementary turbulent flow fields. It was found that the likelihood of fiber entanglement (flocculation) increases in homogeneous turbulence and decreases in turbulence with mean shear or mean strain. The latter two flow fields were also found to have an enhanced probability of inducing floc rupturing (de-flocculation). The concept of a floc yield stress was introduced and a leading-order pipe model for flocculation in developing pipe flow was derived using simple scaling laws and empirical correlations. The aim of this study was to present a few fundamental ideas which may provide a basis for more sophisticated models.

REFERENCES

1. Duffy, G.G. and Lee P.F.W (1978), "Drag reduction in the turbulent flow of wood pulp suspensions", *Appita*, **31**(4), p.280.
2. Taylor, G.I. (1921), "Diffusion by continuous movements", *Proceedings of the London Mathematical Society*, Series 2, **20**, p.196.
3. Fellers, C. and Norman, B. (1998), "Pappersteknik", TABS, 3rd edition, p.84.
4. Tennekes, H. and Lumley, J. L. (1972), "A first course in turbulence", MIT Press, p.230.
5. Kerekes, R.J. (1983), "Pulp floc behavior in entry flow to constrictions", *TAPPI J.*, **66**(1), p.88.
6. Kerekes, R.J., Soszynski, R.M. and Tam Doo, P.A. (1985), "The flocculation of pulp fibres", *Papermaking Raw Materials*, V. Punton Ed., *Transactions of the Eight Fundamental Research Symposium held at Oxford*, Mechanical Engineering Publications Ltd., London, p.265.
7. Bennington, C.P.J., Kerekes, R.J. and Grace, J.R. (1990), "The yield stress of fibre suspensions", *The Canadian Journal of Chemical Engineering*, **68**, p.748.
8. Martinez, D.M., Kiiskinen, H., Ahlman, A-K and Kerekes, R.J. (2003), "On the mobility of flowing papermaking suspensions and its relationship to formation", *Journal of Pulp and Paper Science*, **29**(10), p.341.
9. Ringnér, J. (1999), "Fibre Network Strength and Structure -A Theoretical and Experimental Study-", Licentiate Thesis, Department of Chemical Engineering Design, Chalmers University of Technology, Sweden